Aberrant Epidermal Growth Factor Receptor Signaling and Enhanced Sensitivity to EGFR Inhibitors in Lung Cancer

Joseph Amann,[1] Shailaja Kalyankrishna,[2] Pierre P. Massion,[1] Joyce E. Ohm,[1] Luc Girard,[3] Hisayuki Shigematsu,[3] Michael Peyton,[3] Denise Juroske,[2] Yuhui Huang,[1] J. Stuart Salmon,[1] Young H. Kim,[4] Jonathan R. Pollack,[4] Kiyoshi Yanagisawa,[5] Adi Gazdar,[3] John D. Minna,[3] Jonathan M. Kurie,[2] and David P. Carbone[1]

[1]Vanderbilt-Ingram Cancer Center, Nashville, Tennessee; [2]Department of Thoracic/Head and Neck Medical Oncology, University of Texas M.D. Anderson Cancer Center, Houston, Texas; [3]Hamon Center for Therapeutic Oncology Research, University of Texas Southwestern Medical Center, Dallas, Texas; [4]Department of Pathology, Stanford University School of Medicine, Stanford, California; and [5]Aichi Cancer Center, Nagoya, Japan

Abstract

Epidermal growth factor receptor (*EGFR*) is occasionally amplified and/or mutated in non–small cell lung cancer (NSCLC) and can be coexpressed with other members of the HER receptor family to form functional heterodimers. We therefore investigated lung cancer cell lines for alterations in *EGFR* gene copy number, enhanced expression of EGFR and other HER family members, and EGFR coding sequence mutations and correlated these findings with response to treatment with the EGFR inhibitors and the kinetics of ligand-induced signaling. We show here that somatic deletions in the tyrosine kinase domain of EGFR were associated with increased *EGFR* gene copy number in NSCLC. Treatment with the specific EGFR tyrosine kinase inhibitors (TKI) gefitinib or erlotinib or the EGFR inhibitory antibody cetuximab induced apoptosis of HCC827, a NSCLC cell line with *EGFR* gene amplification and an exon 19 deletion. H1819, a NSCLC cell line that expresses high levels of EGFR, ErbB2, and ErbB3 but has wild-type *EGFR*, showed intermediate sensitivity to TKIs. In both cell lines, ligand-induced receptor tyrosine phosphorylation was delayed and prolonged and AKT was constitutively phosphorylated (but remained inhibitable by EGFR TKI). Thus, in addition to *EGFR* mutations, other factors in NSCLC cells, such as high expression of ErbB family members, may constitutively activate AKT and sensitize cells to EGFR inhibitors. (Cancer Res 2005; 65(1): 226-35)

Introduction

Epidermal growth factor (EGF) receptor (EGFR) expression is readily detectable in ~50% of non–small cell lung cancers (NSCLC; refs. 1, 2), and drugs that inhibit this receptor are under investigation in patients with NSCLC (3). Gefitinib, a p.o. available tyrosine kinase inhibitor (TKI) selective for this receptor, was recently approved for use as second-line therapy for advanced NSCLC based on an objective response rate of ~10% in nonrandomized trials (4, 5). This response rate is less than that of first-line cytotoxic chemotherapy for NSCLC and is similar to that of other second-line chemotherapies. A striking difference between gefitinib and chemotherapy, however, is that the likelihood of response to gefitinib is approximately the same regardless of the number of previous chemotherapy regimens; in contrast, response rates to chemotherapy decrease substantially with each chemotherapy regimen used. In addition, some of the observed responses to gefitinib are dramatic and sustained even in tumors that are completely refractory to cytotoxic chemotherapy, suggesting a unique molecular mechanism of response to gefitinib that is unrelated to mechanisms of response to cytotoxic chemotherapy and still not well understood.

The *EGFR* gene is amplified and overexpressed in a variety of epithelial cancers, including NSCLC (6). More commonly, EGFR protein levels are increased in NSCLC cells through enhanced gene transcription (1). In breast cancer, intratumoral levels of ErbB2 before treatment predict response to treatment with the ErbB2 inhibitory antibody trastuzumab (Herceptin; ref. 7). In these tumors, high levels of ErbB2 correlate with the presence of *ErbB2* gene amplification (7). Although initial immunohistochemical studies indicated that pretreatment levels of intratumoral EGFR do not predict response to gefitinib treatment in NSCLC, there is a close correlation of gefitinib response with the presence of coding sequence alterations in the tyrosine kinase domain of *EGFR* (8, 9). However, data from these studies and others have identified patients whose tumors did not show *EGFR* mutations who nonetheless benefited from gefitinib, suggesting that additional genetic or biochemical factors contribute to gefitinib response in NSCLC (10).

Given the evidence that *EGFR* is amplified and mutated in NSCLC, we investigated whether alterations in copy number or coding sequence correlated with gefitinib response in patients with NSCLC. We identified an amplified *EGFR* gene locus and an in-frame deletion in the *EGFR* kinase domain in the tumors of three patients who had experienced dramatic responses to treatment with gefitinib. In examining NSCLC cell lines, we found that the presence of *EGFR* coding sequence alterations was associated with increased gene copy number, and both *EGFR* gene mutations and high expression of ErbB family members were associated with altered receptor biochemical properties and enhanced sensitivity of NSCLC cells to EGFR TKIs. Particularly striking in gefitinib-sensitive cells was AKT phosphorylation that was independent of exogenous EGF but inhibited by gefitinib, which was associated with prominent apoptotic cell death. Thus, beyond the clear contribution of *EGFR* gene mutations, high expression of ErbB family members, through gene amplification or other mechanisms, with dysregulation of AKT signaling may also contribute to gefitinib sensitivity in NSCLC patients.

Materials and Methods

Reagents. c225 was purchased from the pharmacy at Vanderbilt-Ingram Cancer Center (Nashville, TN). Gefitinib and erlotinib were gifts from AstraZeneca (Wilmington, DE) and OSI Pharmaceuticals (Melville, NY), respectively. Rabbit polyclonal antibodies against pY1068-EGFR, pT202/Y204-ERK, pS473-AKT, total AKT, pY239/Y240-Shc, and total Shc and extracellular signal-regulated kinase (ERK) were purchased from Cell Signaling Technology (Beverly, MA); total EGFR, ErbB2, ErbB3, and ERK1 were from Santa Cruz Biotechnology (Santa Cruz, CA); and pY1148-EGFR and pY845-EGFR were from Biosource International (Camarillo, CA). The anti-EGFR antibody used for immunoprecipitations and Western blotting for total EGFR was a mouse monoclonal antibody obtained from BD Transduction Laboratories (Lexington, KY).

Nomenclature. Two systems for numbering the amino acids of the EGFR were developed. One method numbers each of the amino acids from the methionine from which the protein is translated yielding a protein that is 1,211 amino acids long. The more familiar method used by those who study functional EGFR consider the mature and functional protein to be 1,186 amino acids after processing. All of the antibodies that have been developed for the tyrosine-phosphorylated residues in the cytoplasmic tail use this nomenclature. In attempt to be clear and unambiguous and avoid renumbering all of the known autophosphorylation and Src phosphorylation sites, we have chosen to use the nomenclature for the mature and processed protein.

Cloning of the Mutant EGFR. The mutant EGFR, EGFR Δ722-726, was made by PCR using site-directed mutagenesis by overlap extension (11). Primers used to generate the PCR products were 5′-AATTTCTAGAATGC-GACCCTCCGGGACGGC-3′, 5′-AATTAAGCTTTCATGCTCCAATAAATT--AATTAAGCTTTCATGCTCCAATAAATTCACTGCTTG-3′, 5-GTTAAAATTCCCGTCGCTATCAAAACATCTCCGAAAGCCAACAAGG-3′, and 5′-CCTTGTTGGCTTTCGGAGATGTTTTGATAGCGACGGGAATTT-TAAC-3′. For the first round of PCR, wild-type EGFR in pcDNA3.1 (template) was amplified as follows: 95°C (5 minutes) and 30 cycles of 95°C (1 minute), 58°C (1 minute), and 72°C (3 minutes) followed by extension at 72°C (10 minutes). For the second round, the overlapping products from the first round of PCR were amplified as follows: 95°C (5 minutes) and 30 cycles of 95°C (1 minute), 55°C (1 minute), and 72°C (4 minutes) followed by extension at 72°C (10 minutes). The resulting PCR product containing the mutation was digested with *Bst*XI to release a fragment containing the mutation and subcloned into a *Bst*XI-digested pcDNA3.1/wild-type EGFR construct. Resulting clones were sequenced to verify the presence of the mutation and that no PCR generated mutations were introduced.

DNA Isolation and PCR. DNA was isolated from paraffin-embedded tissues according to the protocol of the Puregene DNA purification kit for such tissues (Gentra Systems, Plymouth, MN). Briefly, paraffin was removed by xylene washes and the tissue was dehydrated with ethanol. Cell lysis buffer was added and cells were mechanically disrupted with a microcentrifuge tube pestle. The resulting lysate was treated with proteinase K overnight at 55°C followed by RNase digestion. Protein was precipitated and removed by centrifugation. DNA was precipitated with isopropanol in the presence of glycogen, washed in 70% ethanol, air dried, and resuspended in DNA hydration solution. DNA was isolated from cell pellets of 1×10^6 to 5×10^6 cells by adding 200 μL of a solution of 25 mmol/L NaOH and 0.2 mmol/L EDTA and heating to 95°C for 20 minutes. This solution was neutralized by the addition of 200 μL of 40 mmol/L Tris-HCl followed by centrifugation at 14,000 rpm at 4°C to pellet insoluble material. The supernatant, which contained the DNA, was used directly for PCR. Primers for PCR were as follows: For exon 19, nested PCR for paraffin-embedded tissues used outside primers 19FWDI (5′-CCATCTCACAATTGCCAGTTA-3′) and 19REV1 (5′-TGCCAGACATGAGAAAAGGTG-3′) and inside primers 19FWD2 (5′-GGATCCCAGAAGGTGAGA-3′) and 19REV2 (5′-ACACAGCAAAGCA-GAAACTC-3′). Only the inside primers were used for PCR of DNA from the NSCLC cell lines. For exon 20, 20FWD (5′-CATGTGCCCCTCCTTCTGG-3′) and 20REV (5′-TATCTCCCCTCCCCGTATCTC-3′) were used. For exon 21, 21FWD (5′-GTTCGCCAGCCATAAGTCCTC-3′) and 21REV (5′-

AGCCTGGTCCCTGGTGTCA-3′) were used. For exons 20 and 21, a second round of PCR was conducted with the same primers as those in the first round of PCR and 1 to 5 μL of the first reaction. PCR for the NSCLC cell lines was done with 1 μL of supernatant and 1 round of PCR. Conditions for the reaction were 95°C (7 minutes) followed by 30 rounds of 95°C (1 minute), 50°C (45 seconds), and 72°C (1 minute) and 1 round of 72°C (10 minutes). PCR products were either purified directly with a PCR purification kit (Qiagen, Valencia, CA) or purified on a 1.6% agarose gel followed by isolation (Qiagen Gel Purification kit). PCR products were sequenced directly with the above PCR primers by submitting purified samples to GenePass, Inc. (Nashville, TN).

Fluorescence *In situ* Hybridization Analysis. Probes specific for EGFR (spectrum orange) and the centromere on chromosome 7 (spectrum green; LSI EGFR/CEP7) were purchased from Vysis, Inc. (Downers Grove, IL). Interphase nuclei were stained by dual-color fluorescence *in situ* hybridization (FISH). For analysis of lung cancer cell lines, cells were centrifuged onto glass slides with a Shandon cytocentrifuge (Thermo Electron Corp., Pittsburgh, PA) and fixed in cold 70% ethanol for 10 minutes followed by fixation for 5 minutes in 85% ethanol and 5 minutes in 100% ethanol. Slides were frozen at −20°C until analysis. Tissue sections were deparaffinized, dehydrated in 100% ethanol, and treated with sodium thiocyanate for 10 minutes at 80°C. Tissues and cell lines were digested with pepsin (4 and 0.5 mg/mL, respectively) in 0.2 N HCl for 10 minutes at 37°C, washed with water, and dehydrated with a graded ethanol series. Slides were then denatured in 70% formamide/2× SSC for 5 minutes at 72°C, dehydrated in graded ethanol, and incubated with a hybridization mixture consisting of 50% formamide, 2× SSC, Cot-1 DNA, and labeled DNA. After 2 nights' incubation at 37°C, the slides were washed at 73°C in 3× SSC (5 minutes), at 37°C in 4× SSC, 0.1% Triton X-100 (5 minutes), and at room temperature in 2× SSC (5 minutes) and counterstained with antifade solution containing 4′,6-diamidino-2-phenylindole. Hybridization signals were scored in 40 nuclei under a ×100 immersion objective. Nuclei in which the nuclear boundaries were broken were excluded from the analysis.

Comparative Genomic Hybridization Microarrays. Array comparative genomic hybridization was done as described previously (14, 15) using 10 μg genomic DNA. Analysis was done using Visual Basic software,[6] which sorts array data according to chromosome location (based on GoldenPath hg16; http://genome.ucsc.edu) and calculates five-point moving average to reduce local variations. The program then generates a color display with red for DNA gain and green for DNA loss.

Cell Lines. NSCLC cell lines were grown in RPMI supplemented with 10% fetal bovine serum (Invitrogen, Carlsbad, CA). Chinese hamster ovary (CHO) cells were maintained in F-12K medium (Invitrogen) supplemented with 10% fetal bovine serum (Hyclone, Logan, UT), 2 mmol/L glutamine, penicillin (100 units/mL), and streptomycin (100 μg/mL, Invitrogen). The 293T cells were grown in DMEM supplemented with 10% fetal bovine serum, 2 mmol/L glutamine, pyridoxine HCl, 110 μg/mL sodium pyruvate, penicillin (100 units/mL), and streptomycin (100 μg/mL). All cells were grown at 37°C in an atmosphere of 5% CO_2.

Western Blot Analysis. For ligand stimulation, NSCLC cells were serum starved overnight. After treatment with EGF for the appropriate periods of time, cells were washed twice with ice-cold PBS, lysed by sonication in radioimmunoprecipitation assay buffer, and stored at −80°C. Protein concentrations were estimated with a Protein Assay kit (Bio-Rad, Hercules, CA), and equal amounts of protein were subjected to SDS-PAGE followed by Western blot analysis with the indicated antibodies and detected by electrochemiluminescence (Amersham Biosciences, Piscataway, NJ).

CHO cells were seeded on 10-cm culture dishes the day before transfection at a density of 2×10^6 cells per plate. Cells were transfected with FuGene 6 (Roche Diagnostics, Indianapolis, IN) according to the manufacturer's instructions with 10 μg DNA and 30 μL FuGene 6 per plate. Medium was replaced 24 hours after transfection followed by serum starvation for 40 to 48 hours after transfection. Cells were starved for 20 to

---

[6] Matrix 1.25, manuscript in preparation.

24 hours before stimulation with 100 ng/mL recombinant human EGF (R&D Systems, Minneapolis, MN) for various periods. Cells were then washed, lysed, sonicated on ice, and centrifuged at 14,000 rpm at 4°C to clarify. Protein was quantified with a DC Protein Assay kit (Bio-Rad) in which 150 μg of lysate, boiled in the presence of SDS-PAGE sample buffer, were run on a Criterion gel (Bio-Rad) followed by transfer onto nitrocellulose. Immunoprecipitations were carried out on 1.5 mg protein lysate by adding 3 μg EGFR monoclonal antibody per lysate and incubating at 4°C, with rocking, for 4 to 6 hours. Protein G-Sepharose (Sigma, St. Louis, MO) and 30 μL of a 50% slurry, blocked with bovine serum albumin, were added to the lysate and incubated for 1 hour at 4°C, with rocking. Beads containing immune complexes were washed thrice with lysis buffer followed by addition of SDS-PAGE sample buffer and boiling for 4 minutes. After separation by SDS-PAGE, proteins were transferred to nitrocellulose, subjected to Western blotting, and visualized by chemiluminescence (Pierce Biotechnology, Rockford, IL).

For 293T cell transfections, cells were plated on 10-cm culture plates at a density of 2.4×10^6 the day before transfection. Cells were transfected with Polyfect (Qiagen) according to the manufacturer's instructions for 293T cells. Serum starvation was initiated 24 hours after transfection and continued for 36 to 42 hours. The appropriate concentrations of gefitinib or erlotinib were added to the culture medium 2 hours before induction with 100 ng/mL EGF for 15 minutes. Cetuximab was added 3 hours before induction. Harvests and transfers were done as described above, except that 100 μg of protein were loaded onto the SDS-PAGE gels.

3-(4,5-Dimethylthiazol-2-yl)-2,5-Diphenyltetrazolium Bromide Assays. Cells were seeded at a density of 1,000 to 5,000 cells per well in 96-well plates and allowed to attach for 24 hours. Cells were then treated with EGFR inhibitors in the presence of 10% serum for 6 days, at the end of which 3-(4,5-dimethylthiazol-2-yl)-2,5-diphenyltetrazolium bromide (MTT) reagent (0.05 mg in PBS) was added to each well. After an incubation of 4 hours, absorbance was read at 570 nmol/L. Values for control cells were considered as 100% viability.

Hoechst 33342 Cell Staining. Control and treated cells were washed gently with PBS, fixed with 4% formaldehyde in PBS at room temperature, washed again with PBS, and incubated with bisbenzimide (Hoechst 33342, 10 μg/mL, Sigma) in PBS for 15 minutes at room temperature. Nuclei were analyzed for chromatin condensation using a fluorescence microscope with an UV filter at a magnification of ×20.

Cell Cycle Analysis. Subconfluent cells in 100-mm dishes were treated with EGFR inhibitors and the supernatants were collected and centrifuged. Adherent cells were trypsinized and pooled with cells from the supernatant. Cell pellets were washed with PBS containing bovine serum albumin, fixed using 70% methanol, and stored at −20°C. The fixed cells were subsequently washed twice with PBS and stained with propidium iodide and RNase A (Phoenix Flow Systems, San Diego, CA), and DNA content was analyzed by flow cytometry. Analyses of 3,000 to 10,000 events were done with a FACScan flow cytometer (Becton Dickinson, San Jose, CA) equipped with a 488-nm argon ion laser and two software packages: CellQuest 3.1 (Becton Dickinson) and ModFit LT 2.0 (Verity Software House, Topsham, ME). Live gating of the forward and orthogonal scatter channels was used to exclude debris and to selectively acquire cell events. DNA area was used to determine the percentage of propidium iodine–stained cells in the sub-G_1 fraction (i.e., apoptotic cells).

Results

Cloning of an *EGFR* Gene Mutation from NSCLC. Tumor cells were isolated from a male, never-smoking patient with bilateral adenocarcinoma. This patient had experienced disease progression through four chemotherapeutic regimens before being given gefitinib as single-agent therapy, which produced rapid and nearly complete tumor shrinkage and remarkable improvement in symptoms. After 18 months, while still taking gefitinib, the patient experienced tumor progression and subsequently died. Sequencing

of the kinase domain of the *EGFR* gene in DNA and RNA isolated from tissue samples taken after treatment as well as from a pre-gefitinib biopsy sample revealed a mutation in exon 19 in both tissue samples (Fig. 1*A*). The mutation consisted of a 15-bp in-frame deletion corresponding to nucleotides 2,235 to 2,249 and resulted in a 5–amino acid deletion [amino acids 722-726 [Δ722-726 mutant)] in the mature protein. DNA was isolated from pretreatment tumor samples of two additional female patients with NSCLC who experienced objective tumor response to gefitinib treatment. One of these patients (patient 2 in Fig. 1*A*) was a never smoker who also presented with bronchioloalveolar carcinoma and had undergone five rounds of chemotherapy before treatment with gefitinib. Patient 3, an ex-smoker (>10 years), was diagnosed with large cell carcinoma of the lung and had received one round of chemotherapy before being treated with gefitinib. These patients relapsed at 8 and 18 months, respectively, while still on gefitinib therapy. Sequence analysis of the EGFR kinase domains in the pretreatment samples revealed similar 15-bp in-frame deletions (Fig. 1*A*).

We examined *EGFR* gene copy number in the lung tumors of the three patients by FISH analysis using probes for *EGFR* and, as a control, the centromere of chromosome 7. The *EGFR* probe detected 6.4, 5.0, and 9.1 copies per cell in tumors from the three patients, and the centromeric probe detected 3.5, 3.8, and 6.8 copies per cell, respectively. Thus, the tumors with *EGFR* mutations also had increased *EGFR* gene copy number, and *EGFR* copy number was increased through a mechanism involving both intrachromosomal gene amplification and chromosomal aneuploidy.

Effects of Ligand on Phosphorylation of EGFR and Downstream Mediators. After binding its ligand, EGFR homodimerizes or heterodimerizes with other ErbB family members, undergoes tyrosine autophosphorylation, and initiates signaling directly through the recruitment of adaptor proteins and intracellular kinases (16). To investigate the effects of the mutation on EGFR function, we cloned and transfected wild-type and mutant receptors into CHO cells, which express low levels of ErbB. Examination of ligand-induced EGFR tyrosine phosphorylation using an anti-phosphotyrosine antibody recognizing all phosphorylated tyrosines revealed that phosphorylation of the mutant receptor was severely impaired when equal amounts of wild-type and mutant protein were compared (Fig. 1*B*). We also examined the kinetics of ligand-induced EGFR phosphorylation on Tyr[1068] and Tyr[1148], which are autophosphorylated, and Tyr[845], which is phosphorylated by Src (Fig. 2*A*). The wild-type receptor was phosphorylated rapidly at these sites, peaking at 10 minutes; by comparison, basal phosphorylation of the mutant receptor was lower at Tyr[845] and Tyr[1068], whereas phosphorylation at Tyr[1148] was approximately equal to wild-type receptor. Ligand-induced phosphorylation of the mutant was delayed at all three sites (peaking at ~2 hours).

We next investigated the kinetics with which ligand-induced EGFR activation induced phosphorylation of downstream mediators (Fig. 2*B*). With the wild-type receptor, Shc phosphorylation peaked between 10 and 30 minutes and declined to barely detectable levels by 6 hours. With the mutant receptor, Shc phosphorylation persisted for longer periods and was still very strong 6 hours post-EGF treatment. In the mutant transfectants, total Shc levels increased with time, which may have contributed to the persistence of Shc phosphorylation. With wild-type EGFR, ERK phosphorylation peaked at 10 minutes and then declined, whereas phospho-ERK levels persisted for longer periods after activation of the mutant EGFR.

Effects of EGFR Inhibitors on Phosphorylation of EGFR and Downstream Mediators. The presence of mutations in most lung tumors that respond to gefitinib suggests that the mutation confers either a unique dependence of the tumor on the EGFR or an increased sensitivity to inhibition by TKIs. To test the sensitivity of the mutant receptor to TKIs, we expressed the wild-type and mutant receptors in 293T cells, which express low levels of other ErbB family members. The transfectants were then treated with TKIs (gefitinib or erlotinib), pulsed with EGF, and subjected to Western analysis. In the absence of EGF, basal phosphorylation at Tyr^{1148}, Tyr^{1068}, and Tyr^{845} was lower in the mutant receptor than in the wild-type receptor (Fig. 3*A*), which is consistent with differences in total EGFR phosphorylation (Fig. 1*B*). After adjusting exposure times to account for differences in basal phosphorylation, IC_{50} values for gefitinib and erlotinib were ~5 to 20 nmol/L for the wild-type receptor and 1 to 5 nmol/L for the mutant receptor at all three phosphorylation sites (Fig. 3*B* and *D*), supporting a 4- to 5-fold increased sensitivity of the mutant receptor to TKIs. However, concerning ERK and Shc phosphorylation, TKI IC_{50} values were similar for the wild-type and mutant receptors (Fig. 3*C*), raising the possibility that other upstream activators maintain the phosphorylation of ERK and Shc in these cells.

EGFR **Gene Amplification and Mutation in NSCLC Cell Lines.** After finding that *EGFR* mutation was associated with gene amplification in NSCLC biopsy samples, we investigated whether this association held true in NSCLC cell lines. For this purpose, we screened eight NSCLC cell lines representing the major histologic subtypes of NSCLC for the presence of *EGFR* gene amplification or
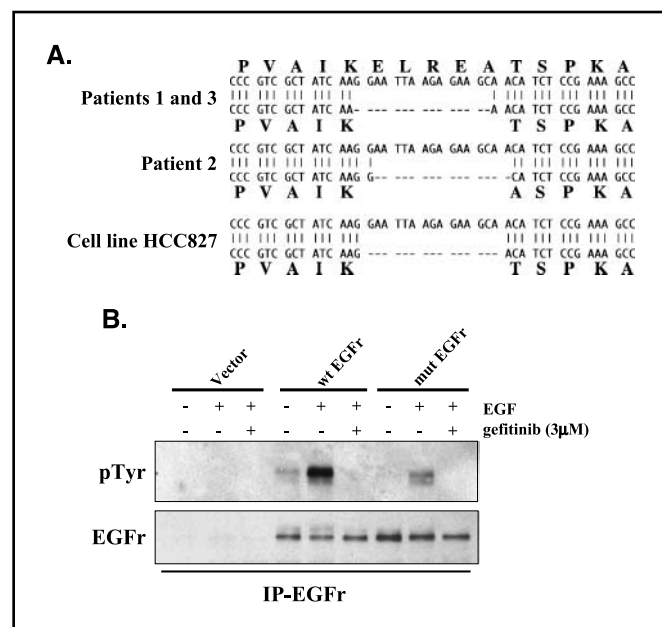

Figure 1. A 15-nucleotide deletion in exon 19 of the EGFR leads to impaired phosphorylation of the exogenously expressed mutated receptor. *A*, sequence of exon 19 from patients who responded to gefitinib and a gefitinib-sensitive cell line reveals in-frame deletions of 15 nucleotides. In addition to the deletion, an amino acid change of threonine to alanine was present in patient 2. *B*, the mutation from patient 1 was subcloned into the full-length receptor (Δ722-726 EGFR), and wild-type (*wt*) or mutated (*mut*) receptor was expressed in CHO cells. Cells were serum starved and treated with EGF or with EGF and gefitinib. Immunoprecipitated EGFR (*IP-EGFr*) was separated on a 7.5% gel by SDS-PAGE followed by phosphotyrosine (*pTyr*) immunoblot to detect total phosphorylated wild-type and mutated receptor. An anti-EGFR immunoblot shows the total amounts of receptor present.
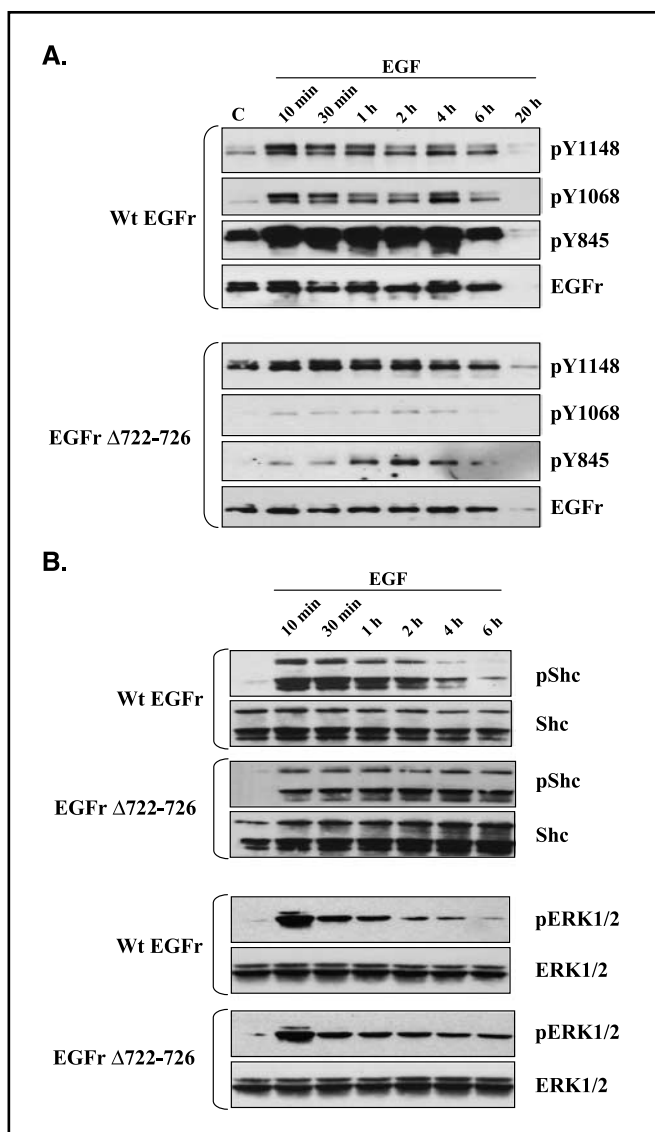

Figure 2. Delayed and sustained phosphorylation of the mutant receptor leads to prolonged phosphorylation of ERK1/2 and high levels of phosphorylated Shc. CHO cells expressing either wild-type (*Wt*) or mutant receptor were serum starved, treated with EGF, and harvested at the indicated times. *A*, wild-type and mutant EGFR were immunoprecipitated from the lysates, separated on a 7.5% gel by SDS-PAGE, and immunoblotted using antibodies specific for various phosphotyrosines. Western blots for each phosphotyrosine antibody and the EGFR antibody are of equal exposure, so phosphorylation between wild-type and mutant can be compared and the differences can be observed. Total amounts of EGFR are also shown. *B*, comparison of the levels of phosphorylated mitogen-activated protein kinases, ERK1/2 (*pERK1/2*), and the adaptor protein Shc (*pShc*) in wild-type and mutant expressing cells. Total lysate (150 μg) was separated on a 10% gel by SDS-PAGE and immunoblotted with the ERK1/2 antibodies and then stripped and reprobed with Shc antibodies.

mutation in exons 19, 20, and 21, the exons most frequently altered in tumors (refs. 8, 9; Table 1). Seven of the cell lines had wild-type *EGFR* gene coding sequences. The eighth cell line, HCC827, established from a 39-year old Caucasian, female, non-smoker had greatly increased *EGFR* gene copy numbers (>20 copies by FISH and 36 copies by comparative genomic hybridization arrays) and a mutation in the *EGFR* coding sequence—a deletion in exon 19 with a resulting amino acid sequence identical to that of our index patient (Fig. 1*A*). Similarly, FISH analysis of H3255, a cell line

shown to have a point mutation in exon 21 (9), was also amplified with >20 copies of the *EGFR* locus (data not shown). H1819, Calu-1, and H1299 cell lines had smaller increases in *EGFR* copy number but no evidence of *EGFR* gene mutations in exons 19, 20, or 21 (all 28 exons were sequenced in H1819 cells). Thus, *EGFR* mutation was associated with high levels of *EGFR* gene amplification in NSCLC cell lines.

ErbB Expression in NSCLC Cell Lines. We next examined the expression of ErbB family members in these eight NSCLC cell lines (Fig. 4*A*). EGFR protein levels were highest in H1819 and HCC827 cells. ErbB2 expression was highest in H1819 cells, which had *ErbB2* gene amplification (8.0 copies per cell by comparative genomic hybridization array), lower in HCC827 cells (which had no evidence of ErbB2 gene amplification), and undetectable in the

other cell lines. ErbB3 was detected in HCC827, H1819, A549, and H226B cells, which had no evidence of *ErbB3* gene amplification. Thus, NSCLC cell lines with increased *EGFR* gene copy number expressed high levels of EGFR and other ErbB family members in part through genetic amplification.

Delayed and Prolonged Phosphorylation of EGFR in NSCLC Cell Lines. After finding that *EGFR* mutation conferred altered phosphorylation of receptor tyrosines in the transfected cells, we compared the levels of phosphorylated EGFR (Y1068) in NSCLC cell lines (Fig. 4*A*). Of the eight cell lines examined under growth conditions, phosphorylation of Y1068 was significantly higher in HCC827 and H1819 cells compared with the other six lines. Although total EGFR levels were also increased in these cell lines, the increase in Y1068 phosphorylation was proportionally greater
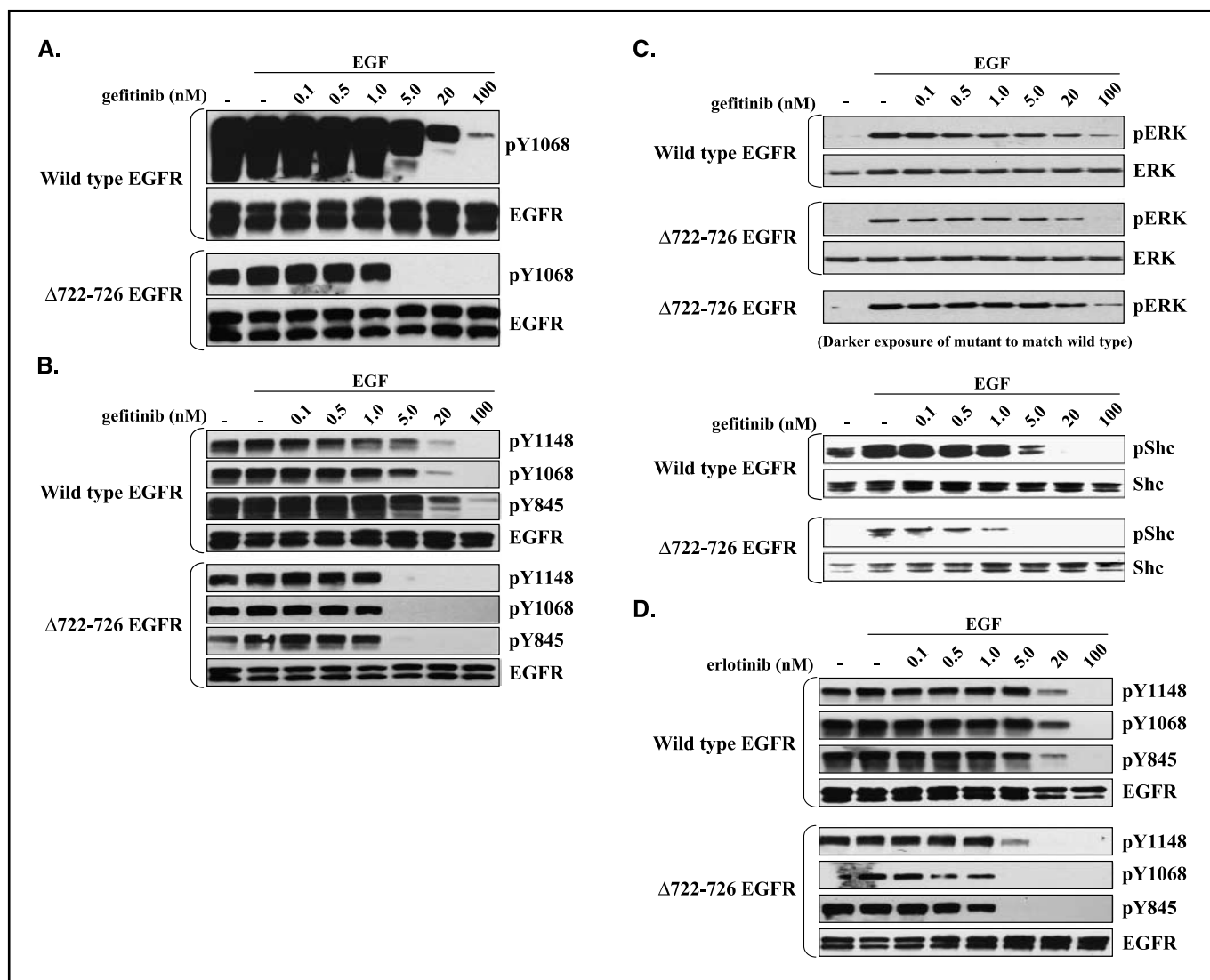

Figure 3. Phosphorylation of the mutated EGFR is more sensitive to the inhibitors gefitinib and erlotinib, whereas the levels of phosphorylated ERK and Shc are unaffected by increasing dose of inhibitor. Wild-type or Δ722-726 EGFR was expressed in 293T cells. Cells were serum starved and treated with increasing doses of gefitinib or erlotinib 2 hours before induction with EGF (100 ng/mL). Total lysate (100 μg) was separated by SDS-PAGE followed by immunoblot with indicated antibodies. *A,* dose curve for gefitinib showing immunoblot for pY1068. As with expression in CHO cells (Fig. 2*A*), there is disparity between phosphorylation of the wild-type and mutant receptor after EGF treatment. *B,* comparison of wild-type and mutant receptor phosphorylation at indicated tyrosines with increasing dose of gefitinib. Exposure times were adjusted to equalize signal for better comparison between phosphorylated tyrosines. *C,* immunoblots showing levels of phosphorylated ERK (*pERK*) and Shc with increasing gefitinib dose. Exposure times of the blots were equivalent for wild-type and mutant transfected cells, except where noted. *D,* dose curves for erlotinib showing phosphorylation of wild-type and mutant receptor at the indicated tyrosines.

Table 1. Characteristics of NSCLC cell lines

Cell line	Gefitinib IC$_{50}$ (μmol/L)	EGFR copy no.	Mutation	Histology
A549	27.6	3.4	−	Adenocarcinoma
H460	28.1	1.1	−	Large cell carcinoma
H226B	17.2	3.1	−	Squamous cell carcinoma
Calu-1	41.0	4.6	−	Squamous cell carcinoma
Calu-6	34.0	2.2	−	Adenocarcinoma
H1299	38.2	3.5	−	Large cell carcinoma
H1819	4.7	5.3	−	Adenocarcinoma
HCC827	0.016	36.0	+	Adenocarcinoma

NOTE: Gefitinib IC$_{50}$ values were calculated from MTT assays done on NSCLC cell lines treated for 6 days, with 16 replicates at each dose. EGFR copy number was measured by FISH analysis, counting signals in at least 25 cells, and mean values are illustrated. For HCC827 cells, we identified 36 copies by array comparative genomic hybridization (copy number was too high to quantitate by FISH). Mutational status of EGFR exons 19, 20, and 21 is indicated as wild-type (−) or mutant (+). Cell lines histologies include adenocarcinoma, squamous cell carcinoma, or large cell carcinoma.

than the increase in total EGFR. H1819 cells also had the highest levels of ErbB2 and ErbB3, which is notable given the presence of multiple phosphatidylinositol 3′-kinase–binding sites on ErbB3.

We next examined the effects of ligand deprivation and ligand stimulation on receptor phosphorylation in these cells. Multiple phosphorylation sites were examined, including Y1068, Y1045, and Y845, with similar results. Therefore, Y1068 was used to represent ligand-induced phosphorylation activity of the EGFR. In addition, all of the resistant cell lines, which showed similar phosphorylation kinetics, will be represented by H1299 in the following experiments. Serum deprivation reduced phosphorylation at Y1068 to undetectable levels in all resistant cell lines and to low, yet detectable, levels in H1819 andHCC827 cells. (Fig. 4B; data not shown). This indicates that EGFR is constitutively phosphorylated in a moderately sensitive cell line (H1819; IC$_{50}$ 4.7 μmol/L) and a very sensitive cell line (HCC827; IC$_{50}$ 0.016 μmol/L). EGF treatment increased phosphorylation at Y1068 in all eight cell lines (Fig. 4B; data not shown). In resistant cells with wild-type EGFR, represented by H1299 (IC$_{50}$ 38.2 μmol/L), an increase in phosphorylated receptor was detected at 30 seconds, peaked at 2 minutes, and began to decline by 30 minutes. In both H1819 and HCC827 cells, an increase was detected at 30 seconds, but instead of declining by 30 minutes, the amount of phosphorylated receptor continued to increase to a maximum level at 1 hour before declining at the 3-hour time point. Thus, both H1819 and HCC827 cells displayed altered kinetics of ligand-induced receptor phosphorylation that was more similar to each other than to the highly resistant cell lines. It is noteworthy that the level of phosphorylation of mutant EGFR at Y1068 in the HCC827 cell line was comparable with the level of phosphorylation of the wild-type receptor in the H1819 cell line (Fig. 4A). This is unlike the decreased levels of Y1068 phosphorylation observed for the mutant receptor in transfected CHO and 293T cells (Figs. 2A and 3A) possibly related to the undetectable levels of wild-type EGFR and low levels of ErbB family members in these cells.

In addition to altered phosphorylation kinetics, there is also a reduced level of receptor turnover in HCC827 and H1819 cells (Fig. 4B). Whereas there is almost a complete down-regulation of total EGFR by 24 hours after ligand stimulation in the H1299 cell line, the level of total EGFR in HCC827 and H1819 remained high. This decreased turnover of receptor may also account for a portion of the higher phosphorylation levels seen in the two sensitive cell lines at later time points.

The phosphorylation of AKT, known to participate in an important survival pathway, was also examined in these cell lines (Fig. 4B). The sensitive cell lines, H1819 and HCC827, showed slight (2-fold maximum) and no induction with ligand, respectively, and were constitutively phosphorylated over the entire time course. The resistant cell line, H1299, on the other hand, was inducible by EGF stimulation and declined to basal levels by 24 hours. Thus, a protein known to be involved in an antiapoptotic pathway is constitutively active in cell lines that show either moderate or high sensitivity to gefitinib.

Sensitivity of NSCLC Cell Lines to EGFR Inhibitors. Given the findings presented here and elsewhere that gefitinib is effective against NSCLC tumors that have *EGFR* gene mutations (8, 9), we investigated whether the antitumor effect of this drug is related to the presence of *EGFR* gene mutation, expression levels of ErbB family members, or both. We also examined the efficacy of erlotinib and cetuximab, an inhibitory antibody against the EGFR ligand-binding domain. We used MTT assays to examine the effect of these agents on the proliferation of NSCLC cells (Fig. 5A; Table 1). Most cell lines with wild-type *EGFR* were relatively resistant to gefitinib, with IC$_{50}$ values of 17.2 to 41.0 μmol/L. However, H1819 cells were moderately sensitive (IC$_{50}$ 4.7 μmol/L) and HCC827 cells were highly sensitive (IC$_{50}$ 10 nmol/L; Table 1). Like gefitinib, erlotinib inhibited the growth of H1819 and HCC827 cells (IC$_{50}$ 5.0 and 0.010 μmol/L, respectively) but not that of H1299 cells (IC$_{50}$ 50.0 μmol/L). Interestingly, cetuximab potently inhibited the growth of HCC827 cells (IC$_{50}$ 7.0 nmol/L) but not H1819 cells (IC$_{50}$ >1.0 μmol/L) or H1299 cells (IC$_{50}$ >1.0 μmol/L; Fig. 5A). Thus, HCC827 cells were uniquely sensitive to agents that target either the EGFR kinase domain or the extracellular domain. Further, the modest sensitivity of H1819 cells to TKIs supports the hypothesis that factors other than *EGFR* gene mutations contribute to the antitumor efficacy of these agents in additional subsets of NSCLC.

We examined HCC827 cells for evidence of apoptosis after treating with EGFR inhibitors (Fig. 5B). Flow cytometry of HCC827 cells treated with gefitinib, erlotinib, or cetuximab showed a hypodiploid peak, representing an increase in the sub-G$_1$ population. Western analysis revealed reductions in the levels of procaspase-3 and

A.

EGFr
ErbB2
ErbB3
pY1068-EGFr
β-actin

A549 H460 H226B Calu1 Calu6 H1299 HCC827 H1819

B.

EGF

C (0) min h C (24h)
0.5 1 2 10 30 1 3 6 24

H1299
H1819   pY 1068-EGFr
HCC827

H1299
H1819   EGFr
HCC827

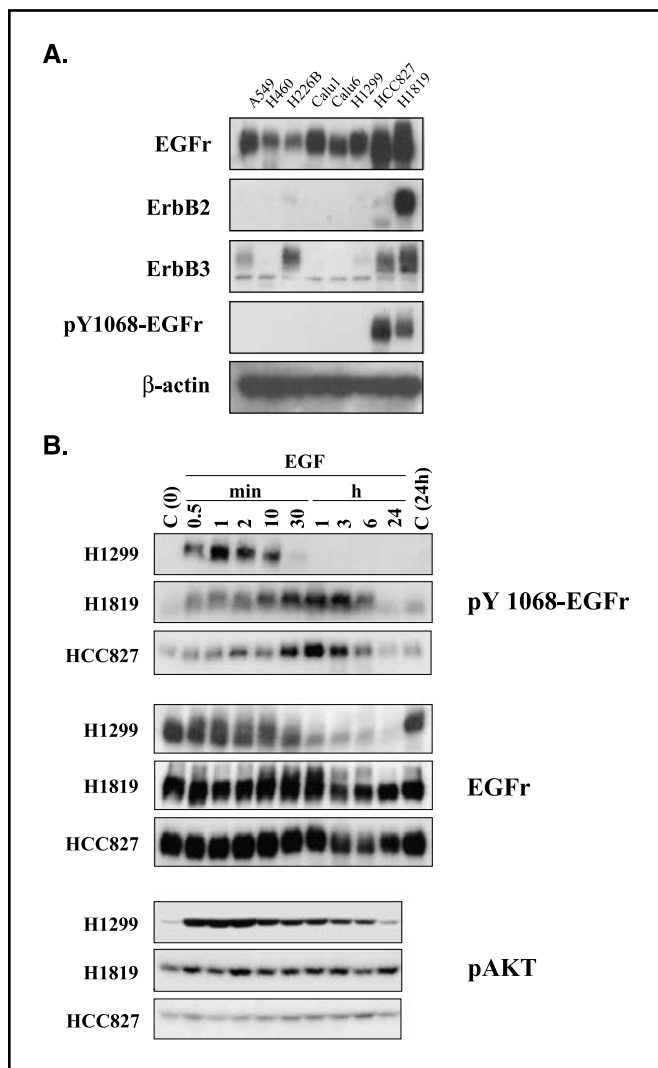H1299
H1819   pAKT
HCC827

Figure 4. Expression of ErbB family members and altered kinetics of ligand-induced phosphorylation of EGFR in NSCLC cell lines. *A,* subconfluent NSCLC cells growing in RPMI with 10% serum were lysed and subjected to Western analysis for detection of total and phosphorylated proteins. *B,* NSCLC cells at 80-100% confluence were serum starved overnight and treated with EGF (50 ng/mL) for the indicated time intervals. Lysates were prepared and EGFR was detected by Western blotting using antibodies to detect site-specific phosphorylation of EGFR (*pY1068-EGFr*), total EGFR (*EGRr*), or phosphorylated AKT (*pAKT*).

poly(ADP-ribose)polymerase (Fig. 5*B*), providing evidence of caspase activation and proteolysis of a caspase-3 substrate. Further, staining of gefitinib-treated HCC827 cells with Hoechst 33342 showed nuclear fragmentation and membrane blebbing (Fig. 5*C*). Together, these findings indicate that HCC827 cells undergo dramatic apoptosis after treatment with EGFR inhibitors.

Finally, we investigated changes in EGFR-dependent signaling following treatment with EGF and EGFR inhibitors. Under serum-starved conditions, AKT is constitutively phosphorylated at high levels and EGF treatment does not further increase phosphorylation in the sensitive cell lines, but a high level of induction was observed in all examined resistant cell lines (Figs. 4*B* and 6*A-C*; data not shown). Treatment with gefitinib (Fig. 6*A*), erlotinib (Fig. 6*B*), or cetuximab (Fig. 6*C*) inhibited basal and EGF-induced phosphoryla-

tion of ERK and AKT in HCC827 cells. EGFR is inhibited by cetuximab in H1819, but phospho-AKT and phospho-ERK are not (Fig. 6*C*), correlating with its failure to respond to this agent. Cetuximab treatment decreased EGFR phosphorylation less prominently in HCC827 cells than in H1819 and H1299 cells. Among these cell lines, HCC827 was the most sensitive with respect to TKI-mediated phosphorylation inhibition of ERK and AKT. Thus, the IC_{50} of the TKIs and cetuximab correlated more closely with the inhibition of ERK and AKT phosphorylation in the three cell types than with receptor autophosphorylation. Interestingly, H1819 and H1299 cells,
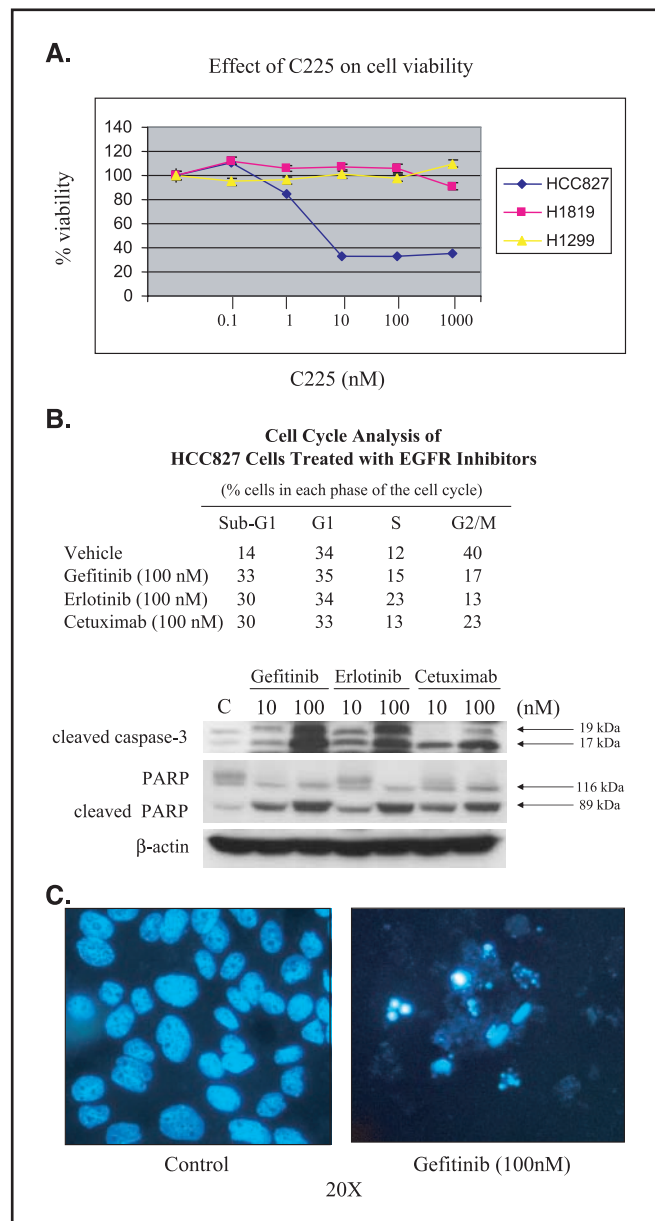
A.

Effect of C225 on cell viability

B.

Cell Cycle Analysis of
HCC827 Cells Treated with EGFR Inhibitors

(% cells in each phase of the cell cycle)

	Sub-G1	G1	S	G2/M
Vehicle	14	34	12	40
Gefitinib (100 nM)	33	35	15	17
Erlotinib (100 nM)	30	34	23	13
Cetuximab (100 nM)	30	33	13	23

Gefitinib Erlotinib Cetuximab
C 10 100 10 100 10 100 (nM)

cleaved caspase-3 → 19 kDa / 17 kDa
PARP → 116 kDa
cleaved PARP → 89 kDa
β-actin

C.

Control   Gefitinib (100nM)
20X

Figure 5. HCC827 cells treated with EGFR inhibitors undergo apoptosis. *A,* HCC827, H1819, and H1299 cells growing in the presence of serum were treated with anti-EGFR Ab (cetuximab) and assayed for viability with MTT assay. *B,* HCC827 cells were treated with TKIs (gefitinib and erlotinib) or anti-EGFR antibody (cetuximab) and evaluated for induction of apoptosis by cell cycle analysis measuring increase in the sub-G_1 population of cells or by Western blotting for detection of caspase-3 and poly(ADP-ribose)polymerase (*PARP*) cleavage. *C,* HCC827 cells stained with Hoechst33342 after treatment with gefitinib for determination of nuclear fragmentation and chromatin condensation.

the TKI IC$_{50}$ values for which differed by a factor of 10, showed similar sensitivities to the TKI-induced inhibition of EGFR phosphorylation, indicating that EGFR phosphorylation was uncoupled from the regulation of cell growth and viability in H1299 cells.

DISCUSSION

We identified deletions in the *EGFR* tyrosine kinase domain from three of three tumors from patients with NSCLC. The *EGFR* genetic alterations, tumor histologies, and smoking histories of these patients were similar to previous reports of patients with NSCLC that responded to gefitinib treatment, with the exception that one patient was diagnosed with large cell carcinoma (8, 9). We also identified *EGFR* mutations in HCC827 cells and two other NSCLC cell lines not reported previously,[7] involving in-frame deletions and point mutations similar to the spectrum of changes in NSCLCs with *EGFR* mutations described previously (8, 9). To date, these *EGFR* gene mutations have been found less often in NSCLC in people who were smoking at diagnosis, suggesting that the genetic basis of lung tumorigenesis in such individuals is distinct from that
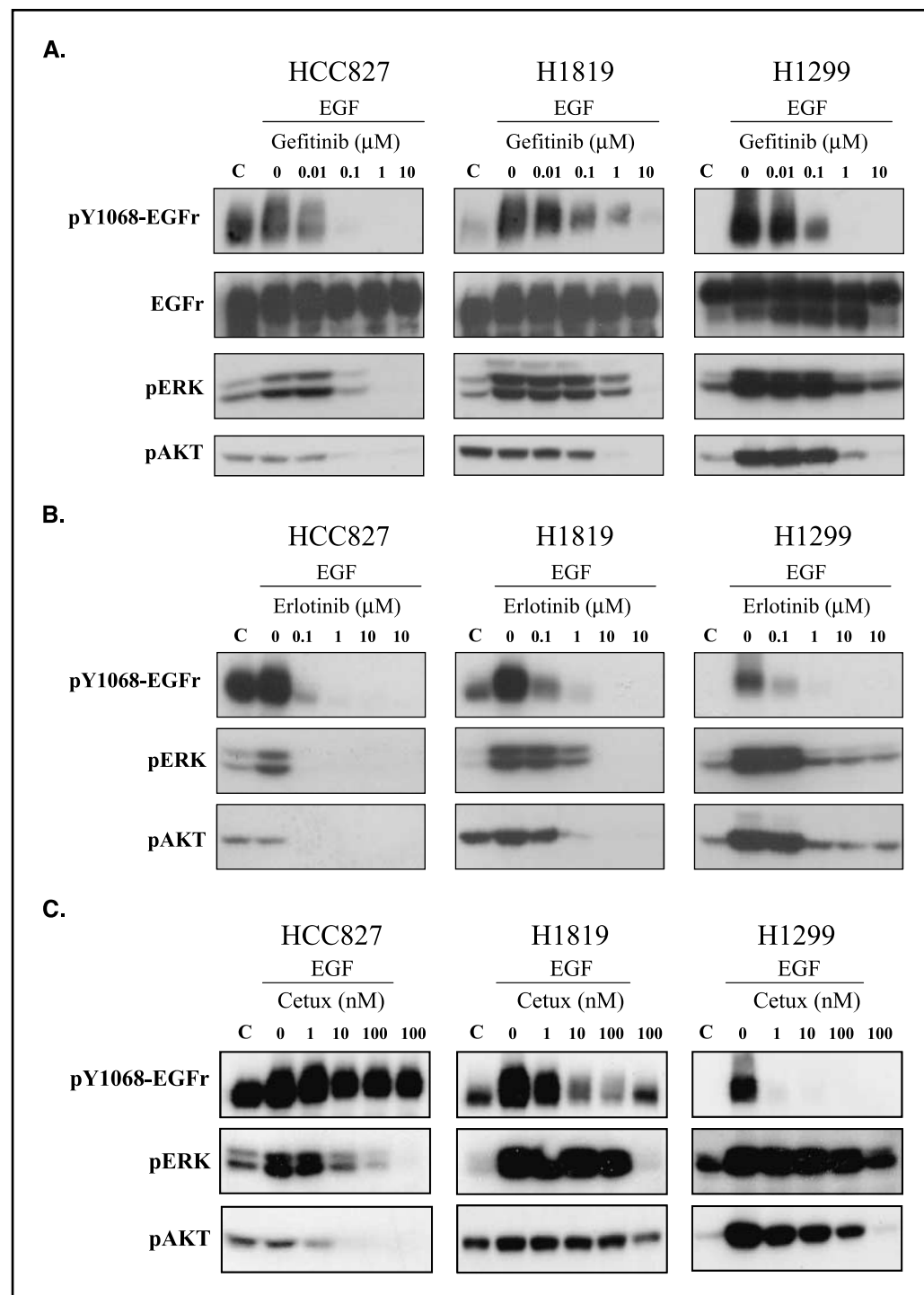

Figure 6. Inhibition of EGF-induced phosphorylation of EGFR, ERK, and AKT by gefitinib, erlotinib, and cetuximab. HCC827, H1819, or H1299 cells were pretreated with (*A*) gefitinib for 2 hours, (*B*) erlotinib for 3 hours, or (*C*) cetuximab (*Cetux*) for 3 hours and treated with EGF for 60 minutes (for HCC827 and H1819) and 5 minutes (for H1299; to coincide with the peak timing of EGFR activation in these cells). Lysates were probed for phosphorylated and total proteins by Western blot analysis. Western analysis for actin levels revealed equal loading of the wells (data not shown).

of people who either had never smoked or had quit smoking. The frequency of NSCLC among former smokers has increased over the past decade, with former smokers now accounting for >50% of all NSCLC cases. Thus, elucidating the molecular basis of lung cancer in this subgroup has tremendous public health implications.

We found that *EGFR* mutations were associated with an increased number of *EGFR* gene copies (three of three tumors and four of four cell lines), raising the possibility that the process of genetic instability that caused *EGFR* gene amplification also facilitated the development of coding sequence mutations or amplified their effect. In the four cell lines containing mutations, including HCC827 and H3255, reported previously to have the L858R point mutation, FISH analysis indicated that the *EGFR* locus was highly amplified by intrachromosomal duplication and contained anywhere from 12 to >20 *EGFR* loci (Table 1; data not shown; ref. 9). Seven cell lines that contained wild-type EGFR were also examined by FISH, and although many were aneuploid, none contained >5 *EGFR* loci on average (Table 1) and, more importantly, none showed evidence of intrachromosomal duplication. These data combined with the patient data showing amplification of the *EGFR* locus increase the likelihood that *EGFR* mutational events may depend on the specific process driving genetic instability in NSCLC.

The mutant receptor also displayed altered biochemical properties. Our transfection studies in CHO and 293T cells revealed that the overall phosphorylation level of the mutant receptor was lower than that of the wild-type receptor. This is in agreement with the studies of Pao et al., who also used 293T cells for transfections, but differ from the other two studies where Cos7 and mouse mammary epithelial cells were used (8, 17, 18). Monitoring the levels of phosphorylation of specific tyrosines in the mutant transfected cells revealed large differences between mutant and wild-type receptor. For example, in CHO cells, the phosphorylation of Y1148 was at or near wild-type levels, whereas Y1068 and Y845 were much reduced when compared with wild-type (Fig. 2*A*). Sordella et al. also noted differences in tyrosine phosphorylation; however, the specific tyrosine phosphorylation in the mutant stable transfectants was usually higher. This is most likely due to higher levels of wild-type EGFR or other ErbB family members. Basal tyrosine phosphorylation in HCC827 (this study) and H3255 (9) NSCLC cells was also increased relative to that of cells with wild-type receptor. This discrepancy between transfected CHO and 293T cells and NSCLC cell lines containing a mutation is most likely a consequence of the low levels of endogenous ErbB present in CHO and 293T cells, which limit the dimeric partners with which the transfected EGFR could interact. HCC827 cells and H1819 cells expressed high levels of ErbB2 and ErbB3, which can dimerize with EGFR and potentially enhance its phosphorylation. In fact, overexpression of ErbB2 has been shown to promote constitutive phosphorylation of EGFR and to delay and prolong the phosphorylation of the receptor (19). Importantly, the use of the C225 mouse monoclonal antibody was unable to eliminate constitutive phosphorylation of the EGFR, implicating overexpression of ErbB2, and not EGF binding, as the most likely reason for the enhanced signaling through the EGFR. These results recapitulate exactly what is seen in the H1819 cell line including the inability of cetuximab to eliminate constitutive phosphorylation of the EGFR. In that study (19), it was determined that the reason for the prolonged signaling

<hr>

[7] Manuscript in preparation.

was due to altered trafficking and thus decreased down-regulation of the receptor. It will be interesting to see if in future studies the mutations associated with the enhanced sensitivity to gefitinib and erlotinib also affect trafficking of the EGFR.

Additional factors may contribute to the changes in the kinetics of phosphorylation, including interaction of the receptor with phosphatases. Previous studies, using time courses of 30 to 180 minutes after ligand stimulation, have shown peak phosphorylation of mutant EGFR by 2 to 3 hours in transfected cells without diminution of signal (8, 17, 18). This suggests that interaction of the mutated receptor with phosphatases may be altered. We have monitored phosphorylation of the receptor for up to 24 hours after ligand stimulation and noted a peak of 2 to 3 hours followed by decreased phosphorylation at 4 to 6 hours post-stimulation, indicating the mutated receptor can still interact with and be dephosphorylated by phosphatases. Importantly, the same kinetics is seen in the H1819 cells, which do not have a mutated receptor. This result argues that mutation is not altering the association of the receptor with phosphatases and that some other mechanism of receptor down-regulation is being affected.

Downstream targets of the mutated receptors have also been examined in one study using a 30-minute time course post-ligand stimulation (17). It was determined that ERK1/2 phosphorylation in stably transfected cells was no different whether cells contained mutant or wild-type receptor. In our studies, we also do not see a change in the phosphorylation pattern of ERK1/2 by 30 minutes, but by 2 hours there is a higher level of phosphorylated ERK1/2 in the cells transfected with mutant receptor when compared with lysates from cells transfected with wild-type receptor. Because the ERK1/2 signaling pathway is an important proliferation pathway, prolonged phosphorylation of this protein may have profound effects on the growth characteristics of cells that contain the mutation as is seen in the cell lines harboring the mutation that are grown in the presence of EGF (17). Shc, a direct target of the EGFR and upstream activator of the Ras/mitogen-activated protein kinase pathway, as expected, is also phosphorylated for a prolonged period of time. Thus, our results are consistent with an up-regulated proliferation pathway involving the Ras oncogene and mitogen-activated protein kinase signaling.

Lastly and perhaps most importantly, AKT was constitutively phosphorylated in HCC827 and H1819 cells (characterized by persistent AKT phosphorylation in the serum-starved state and lack of response to ligand stimulation), but both cell types retained phospho-AKT sensitivity to TKIs. Our findings differed from those of a recent report in which EGF increased AKT phosphorylation in NSCLC cells with mutant EGFR (17). The biological basis for this difference is not clear but may be related to the different cell lines used in the two studies, which had different *EGFR* mutations and may vary in the expression levels of ErbB family members (particularly ErbB3), which can directly or indirectly activate phosphatidylinositol 3'-kinase.

Treatment with EGFR inhibitors also revealed biochemical differences between mutant and wild-type receptor. Our mutant receptor was more sensitive than the wild-type to TKI-induced inhibition of EGFR phosphorylation, a finding consistent with previous reports (8, 9). However, the resistance of NSCLC cells with wild-type EGFR to growth inhibition by TKIs was not simply a consequence of reduced EGFR sensitivity to drug. Relative to H1299 cells, HCC827 cells showed a 2,500-fold increased sensitivity to TKI-induced inhibition of growth but only a 10-fold increased sensitivity to EGFR phosphorylation, raising the possibility that the mechanism of

resistance to TKIs in NSCLC cells without *EGFR* mutations is downstream of EGFR. If proven true, this hypothesis has clinical consequences; increasing the dose of TKIs given to patients with NSCLC without *EGFR* mutations will not be clinically effective. Other features of the tumor such as increased *EGFR* copy number, coexpression of other ErbBs, or specific aspects of receptor signaling may better predict relative sensitivity in tumors with wild-type receptor. TKI-induced inhibition of AKT and ERK phosphorylation correlated closely with the IC_{50} values of the TKIs in these cells, supporting recent (17) and previous (20, 21) reports that AKT is a crucial mediator of EGFR-induced cell survival and clinical response. It is interesting to note that the tumor from patient 1 in our study who developed clinical resistance to gefitinib continued to express high levels of the mutant EGFR protein (data not shown), implying the acquisition of mechanisms to bypass the apoptotic response.

Like the authors of previous reports (8, 9), we observed a striking association of *EGFR* coding region alterations with enhanced sensitivity to treatment with TKIs. HCC827 cells underwent apoptosis in response to treatment with TKIs, demonstrating that EGFR activation was required for the survival of these cells. Further, HCC827 cells also underwent apoptosis in response to cetuximab treatment, indicating that the apoptotic response was not simply a consequence of enhanced affinity of mutant EGFR for TKIs; instead, it reflects a dependence of the cells on EGFR activity for survival. Moreover, H1819 cells were also sensitive to treatment with TKIs, albeit to a lesser extent than HCC827 cells, supporting the hypothesis that factors other than *EGFR* mutations, such as expression levels of other ErbBs, also sensitized NSCLC cells to TKIs. It is paradoxical that cetuximab did not reduce the phosphorylation of AKT in H1819 cells and result in cell death like the TKIs. It is likely that overexpression of ErbB2, which makes cells with wild-type receptor sensitive to the TKIs, is the reason why the H1819 cells are refractory to the treatment with cetuximab. The constitutively active EGFR/ErbB2 heterodimer most likely remains at the surface for a longer period of time than the EGFR homodimer (18) and it is at the cell surface where signaling through phosphatidylinositol 3′-kinase seems to occur (22). This interpretation of the cetuximab finding again reinforces the importance of AKT signaling on cell survival.

These findings have potential clinical applications. *EGFR* gene mutations have not been detected in patients with NSCLC who experience stable disease after erlotinib treatment (23). However, erlotinib treatment prolonged the survival of such patients. Thus, we hypothesize that, in response to treatment with TKIs, most NSCLCs with *EGFR* gene mutations will undergo tumor shrinkage, whereas tumors that have no *EGFR* mutations but express high levels of other ErbB family members (through gene amplification or other mechanisms) may respond or exhibit stability of disease, conferring clinically meaningful benefit. In addition, these studies suggest that coadministration of gefitinib or erlotinib with specific ErbB2 inhibitors may prove useful in NSCLC where both EGFR and ErbB2 are overexpressed.

References

1. Rusch V, Baselga J, Cordon-Cardo C, et al. Differential expression of the epidermal growth factor receptor and its ligands in primary non-small cell lung cancers and adjacent benign lung. Cancer Res 1993;53:2379–85.
2. Rusch V, Klimstra D, Linkov I, Dmitrovsky E. Aberrant expression of p53 or the epidermal growth factor receptor is frequent in early bronchial neoplasia and coexpression precedes squamous cell carcinoma development. Cancer Res 1995;55:1365–72.
3. Baselga J, Albanell J. Epithelial growth factor receptor interacting agents. Hematol Oncol Clin North Am 2002;16:1041–63.
4. Fukuoka M, Yano S, Giaccone G, et al. Multi-institutional randomized phase II trial of gefitinib for previously treated patients with advanced non-small-cell lung cancer. J Clin Oncol 2003;21:2237–46.
5. Kris MG, Natale RB, Herbst RS, et al. Efficacy of gefitinib, an inhibitor of the epidermal growth factor receptor tyrosine kinase, in symptomatic patients with non-small cell lung cancer: a randomized trial. JAMA 2003;290:2149–58.
6. Hirsch FR, Varella-Garcia M, Bunn PA Jr, et al. Epidermal growth factor receptor in non-small-cell lung carcinomas: correlation between gene copy number and protein expression and impact on prognosis. J Clin Oncol 2003;21:3798–807.
7. Cobleigh MA, Vogel CL, Tripathy D, et al. Multinational study of the efficacy and safety of humanized anti-HER2 monoclonal antibody in women who have HER2-overexpressing metastatic breast cancer that has progressed after chemotherapy for metastatic disease. J Clin Oncol 1999;17:2639–48.

8. Lynch TJ, Bell DW, Sordella R, et al. Activating mutations in the epidermal growth factor receptor underlying responsiveness of non-small-cell lung cancer to gefitinib. N Engl J Med 2004;350:2129–39.
9. Paez JG, Janne PA, Lee JC, et al. EGFR mutations in lung cancer: correlation with clinical response to gefitinib therapy. Science 2004;304:1497–500.
10. Shepherd FA, Periera J, Ciuleanu TE, et al. A randomized, placebo-controlled trial of erlotinib in patients with advanced non-small cell lung cancer following failure of 1st line or 2nd line chemotherapy [abstract 7022]. Proc Am Soc Clin Oncol 2004.
11. Ho SN, Hun HD, Horton RM, Pullen JK, Pease LR. Site-directed mutagenesis by overlap extension using the polymerase chain reaction. Gene 1989;77:51–9.
12. Liu S, Liu W, Jakubczak JL, et al. Genetic instability favoring transversions associated with ErbB2-induced mammary tumorigenesis. Proc Natl Acad Sci U S A 2002;99:3770–5.
13. Montagna C, Andrechek ER, Padilla-Nash H, Muller WJ, Ried T. Centrosome abnormalities, recurring deletions of chromosome 4, and genomic amplification of HER2/*neu* define mouse mammary gland adenocarcinomas induced by mutant HER2/*neu*. Oncogene 2002;21:890–8.
14. Pollack JR, Perou CM, Alizadeh AA, et al. Genome-wide analysis of DNA copy-number changes using cDNA microarrays. Nat Genet 1999;23:41–6.
15. Pollack JR, Sorlie T, Perou CM, et al. Microarray analysis reveals a major direct role of DNA copy number alteration in the transcriptional program of human breast tumors. Proc Natl Acad Sci U S A 2002;99:12963–8.

16. Schlessinger J. Ligand-induced, receptor-mediated dimerization and activation of EGF receptor. Cell 2002;110:669–72.
17. Sordella R, Bell DW, Haber DA, Settleman J. Gefitinib-sensitizing EGFR mutations in lug cancer activate anti-apoptotic pathways. Science 2004;304:. Epub 2004 Jul 29.
18. Pao W, Miller V, Zakowski M, et al. EGF receptor gene mutations are common in lung cancers from "never smokers" and are associated with sensitivity of tumors to gefitinib and erlotinib. Proc Natl Acad Sci U S A 2004; 101:13306–11.
19. Worthylake R, Opresko LK, Wiley HS. ErbB-2 amplification inhibits down-regulation and induces constitutive activation of both ErbB-2 and epidermal growth factor receptors.
20. Bianco R, Shin I, Ritter CA, et al. Loss of PTEN/MMAC1/TEP in EGF receptor-expressing tumor cells counteracts the antitumor action of EGFR tyrosine kinase inhibitors. Oncogene 2003;22:2812–22.
21. She QB, Solit D, Basso A, Moasser MM. Resistance to gefitinib in PTEN-null HER-overexpressing tumor cells can be overcome through restoration of PTEN function or pharmacologic modulation of constitutive phosphatidylinositol 3′-kinase/Akt pathway signaling. Clin Cancer Res 2003; 9:4340–6.
22. Wiley HS. Trafficking of the ErbB receptors and its influence on signaling. Exp Cell Res 2003;284:78–88.
23. Herbst RS, Prager D, Hermann R, et al. TRIBUTE—a phase III trial of erlotinib HCl combined with carboplatinum and paclitaxel chemotherapy in advanced non-small cell lung cancer [abstract 7011]. Proc Am Soc Clin Oncol 2004.

Aberrant Epidermal Growth Factor Receptor Signaling and Enhanced Sensitivity to EGFR Inhibitors in Lung Cancer

Joseph Amann, Shailaja Kalyankrishna, Pierre P. Massion, et al.

Updated version	Access the most recent version of this article at: http://cancerres.aacrjournals.org/content/65/1/226

Cited articles	This article cites 19 articles, 10 of which you can access for free at: http://cancerres.aacrjournals.org/content/65/1/226.full#ref-list-1
Citing articles	This article has been cited by 88 HighWire-hosted articles. Access the articles at: http://cancerres.aacrjournals.org/content/65/1/226.full#related-urls

E-mail alerts	Sign up to receive free email-alerts related to this article or journal.
Reprints and Subscriptions	To order reprints of this article or to subscribe to the journal, contact the AACR Publications Department at pubs@aacr.org.
Permissions	To request permission to re-use all or part of this article, use this link http://cancerres.aacrjournals.org/content/65/1/226. Click on "Request Permissions" which will take you to the Copyright Clearance Center's (CCC) Rightslink site.